

MiR-138-5p predicts negative prognosis and exhibits suppressive activities in hepatocellular carcinoma HCC by targeting FOXC1

G. YANG, S. GUO, H.-T. LIU, G. YANG

Clinical Laboratory, Zhongnan Hospital of Wuhan University, Wuhan, Hubei, China

Abstract. – **OBJECTIVE:** Accumulating evidence verified that microRNAs (miRNAs) participate in the development of several cancers.

PATIENTS AND METHODS: The levels of miR-138-5p and forkhead box c1 (FOXC1) were examined using quantitative Real-time PCR (qRT-PCR). Cell Counting Kit-8 (CKK-8), colony formation, migration, and Transwell invasion assays were conducted to examine the impact of miR-138-5p on hepatocellular carcinoma (HCC) cells. The protein expression of FOXC1 was detected using Western blotting assay. The tumor growth of HCC cell *in vivo* was analyzed using transplanted tumor model. The expressions of FOXC1 and Ki67 *in vivo* were assessed using immunohistochemistry (IHC) assay.

RESULTS: We testified that miR-138-5p was down-expressed in HCC and the low level of miR-138-5p was related to the poor clinical outcome of patient with HCC. Moreover, miR-138-5p repressed the growth and metastatic phenotypes of HCC cells. Consistent with the results *in vitro* investigations, we revealed that miR-138-5p served as a suppressive miRNA in the growth of HCC cell *in vivo*. By using the luciferase assay and immunoblotting, we validated that FOXC1 was a potential downstream gene of miR-138-5p. Finally, our results showed that re-expression of FOXC1 rescued the growth and metastatic-related traits of HCC cell inhibited by miR-138-5p.

CONCLUSIONS: Altogether, our observations imply that miR-138-5p restrains the aggressive phenotypes of HCC cell *via* modulating FOXC1.

Key Words:

HCC, MiR-138-5p, FOXC1, Migration, Invasion.

Introduction

Hepatocellular carcinoma (HCC) is still a lethal malignancy and the primary cause of cancer related mortality worldwide. Owing to the great advances in the treatments, the overall survival

of patients with HCC have improved. However, the five-year survival rate of patients with HCC is less than 5%. Local diffusion and distant metastases are the main reasons for the poor clinical outcome of HCC. Hence, further investigations of exact mechanisms are necessary and helpful to explore effective treatment options for anticancer therapy.

MicroRNAs (miRNAs) are small noncoding RNAs which suppress mRNAs translation and/or negatively modulate the stability mRNAs through interaction with the 3'-untranslated regions (3'-UTRs) of their target genes^{1,2}. In malignancies, miRNAs act as either anti-oncogenes or cancer-promoting genes. MiRNAs participate in numerous biological processes of cancers, including cell proliferation, metastasis and apoptosis. In particular, miR-194 deregulation induces the growth and metastases of colorectal carcinoma cell *via* targeting serine/threonine kinase 2 (AKT2)³. MiR-143-3p acts as a tumor suppressive miRNA through regulating the growth, invasiveness and the epithelial-mesenchymal transition (EMT) through targeting KH Domain Containing RNA Binding-5 (QKI-5) in esophageal squamous cell carcinoma (ESCC)⁴. Downregulation or overexpression of miR-138 has been shown to play crucial actions in regulating the aggressiveness of cancers, including lung cancer, leukemia and pancreatic cancer. Besides, miR-138-5p has been proved to contribute to the proliferation and invasion of bladder cancer cells by targeting surviving⁵. Of note, miRNA-138-5p regulates the proliferation of pancreatic carcinoma cell *via* directly regulating FOXC1. Nevertheless, the exact role of miR-138-5p in HCC development is still largely unknown. Also, the precise underlying molecular mechanisms through which miR-138-5p regulates HCC metastasis remains largely unknown

and deep explorations are needed. In the current study, we demonstrated that miR-138-5p was strikingly down-expressed in both clinical HCC samples and liver cancer cells. Transfection of miR-138-5p markedly impaired the growth, migrate and invasive abilities of HCC cell *in vitro*. In addition, miR-138-5p significantly repressed HCC cell growth *in vivo*. Specifically, we reported that FOXC1 was a functional target of miR-138-5p in HCC. MiR-138-5p inhibited the proliferation and aggressive phenotypes of HCC cell *via* downregulation of FOXC1. Our findings implied that miR-138-5p/FOXC1 axis was a vital element of HCC growth and metastasis.

Patients and Methods

Tissue Samples

48 cases of HCC samples and adjacent non-cancerous tissues were collected from the Zhongnan Hospital of Wuhan University were stored at -80°C. The study was approved by the Ethics Committee of Zhongnan Hospital of Wuhan University (Approval No. ZHWU20170911) and the written informed consent was obtained from

patients before this study. The patients' characteristics are presented in Table I.

Cell Culture

The human HCC cell lines PLC/PRF/5, HepG2, SMMC-7721 and HuH7 as well as human normal hepatocytes (LO2 cell) were bought from Nanjing Keygen (Nanjing, Jiangsu, China). HCC cells were maintained using RPMI-1640 and LO2 cell was cultured in Dulbecco's Modified Eagle's Medium (DMEM) containing 10% fetal bovine serum (FBS) in a humidified atmosphere of 5% CO₂ at 37°C.

In Situ Hybridization (ISH) of miR-138-5p

Locked nucleic acids (LNA)-modified probe was 5' labeled with digoxigenin (Qiagen, Hilden, Germany). After 15 µg/ml proteinase K digestion, 30 nM of the probes were hybridized to HCC tissues for 15 hours at 62°C. The probe target was detected using alkaline phosphatase activity on the nitroblue tetrazolium and bromochloroindoyl phosphate substrate followed by Nuclear Red counterstain.

Table I. Relationship between the expression of miR-138-5p and clinicopathological parameters in patients with HCC.

Parameter	miR-138-5p		p-value
	High	Low	
Age (years)			0.078
< 50	16	12	
> 50	9	11	
Gender			0.106
Male	18	14	
Female	10	6	
Tumor size (cm)			0.143
< 5	14	16	
≥ 5	8	10	
TNM stage			0.004
I-II	19	10	
III-IV	5	14	
AFP (ng/mL)			0.083
< 400	12	11	
≥ 400	15	10	
Differentiation			0.248
Poorly	20	7	
Moderately well	9	12	
Distant Metastasis			0.031
Positive	3	13	
Negative	13	19	

Cells Transfection

MiRNA-138-5p mimics, miR-138-5p inhibitor (anti-miR-138-5p), miRNA negative control (miR-NC), small interfering RNA (siRNA) negative control and siRNA targeting FOXC1 (si-FOXC1) were obtained from RiboBio (Guangzhou, Guangdong, China). MiRNA-138-5p mimics were transfected into HCC cells by using Lipofectamine 2000 (Thermo Fisher Scientific, Waltham, MA, USA) for 48 hours. To increase the level of FOXC1, the full-length sequence of FOXC1 was constructed by GeneCopoeia (Guangzhou, Guangdong, China) and was inserted into pcDNA3.1 vector (RiboBio).

qRT-PCR Assay

Total RNAs were isolated using TRIzol kit (Thermo Fisher Scientific, Waltham, MA, USA). The miScript Reverse Transcription kit (Qiagen, Hilden, Germany) was used to construct complementary DNA (cDNA) from total RNAs. Then, the cDNA was amplified by using a miScript SYBR Green PCR kit (Qiagen, Hilden, Germany) on a Roche Light Cycler 480 Real-Time PCR System (Roche Diagnostics, Basel, Switzerland). To quantify FOXC1 mRNA level, reverse transcription was conducted using a PrimeScript RT Reagent Kit (TaKaRa Biotechnology, Dalian, China). After that, qRT-PCR was carried out using a SYBR Premix Ex Taq™ Kit (TaKaRa Biotechnology, Dalian, China). The sequences of the primers were listed as follows: miR-138-5p forward primer 5'-GCGAGCTGGT-GTTGTGAATC-3' and reverse primer 5'-AGTG-CAGGGTCCGAGGTATT-3'; U6 forward primer 5'-AAAGCAAATCATCGGACGACC-3' and reverse primer 5'-GTACAACACATTGTTTCCTC-GGA-3'; GAPDH forward primer 5'-AATGGA-CAACTGGTCGTGGAC-3' and reverse primer 5'-CCCTCCAGGGGATCTGTTT-3'; FOXC1 forward primer 5'-GGCGAGCAGAGCTAC-TACC-3' and reverse primer 5'-TGCGAGTA-CACGCTCATGG-3'; RARA forward primer 5'-AAGCCCGAGTGCTCTGAGA-3' and reverse primer 5'-TTCGTAGTGTATTTGCCAGC-3'. Small nuclear RNA U6 and GAPDH were endogenous controls. All results were analyzed using $2^{-\Delta\Delta Ct}$ method.

Luciferase Reporter Gene Assay

The 3'-UTR fragments of FOXC1 containing wild-type (wt) or mutant type (mut) miR-138-5p binding sites were produced by GeneCopoeia (Guangzhou, Guangdong, China) and inserted

into pmirGLO luciferase reporter gene (Promega, Madison, WI, USA), and named as FOXC1-Wt or FOXC1-Mut. HCC cell was cultured in 24-well plates and transfected with plasmid combination with miR-138-5p by using Lipofectamine 3000. After 48 hours, the luciferase activities were analyzed using luciferase reporter system (Promega, Madison, WI, USA)

Proliferation Assay

Cells (5×10^3 per well) were cultured into 96-well plates and cultured for 24 hour, 48 hour, 72 hours or 96 hours, respectively. After each time point, CCK-8 solution was added to the plates. Cells were incubated for four hours and the optical density (OD) was assessed at 450 nm under a micro-plate reader (BioRad, Hercules, CA, USA).

Colony Formation

HCC cells (1×10^3) were seeded in six well plates. The cell colonies were stained using crystal violet (0.1%) after two weeks. The number of colonies (more than 50 cells) was counted.

Migration Analysis

HCC cells (3×10^5) were plated into 6 well plates. After 24 hours, straight wounds were made using 100 μ l pipette tip. The width of the wound gap was recorded under an inverted microscope and photographed at 0 hour or 24 hours, respectively.

Invasion Assay

The upper chamber of 8- μ m pore size Transwell plate (Corning, MA, USA) was coated with Matrigel. 200 μ l of HCC cells (5×10^4) was added into the upper compartment and 500 μ l of culture medium containing 20% FBS was plated into the lower compartment. 24 hours later, invaded HCC cells were stained using crystal violet (1%) and counted.

Immunoblotting

Whole-cell lysates were prepared using radio-immunoprecipitation assay (RIPA) buffer. 30 μ g proteins were separated using 10% sodium dodecyl sulfate polyacrylamide gel electrophoresis (SDS-PAGE) and then transferred onto polyvinylidene difluoride (PVDF) membrane. After blocking using 5% BSA, the PVDF membrane was incubated with FOXC1 or GAPDH antibody (Santa Cruz Biotechnology, CA, USA) overnight. After that, the PVDF membrane was incubated

with horseradish peroxidase (HRP)-conjugated goat-anti-rabbit IgG antibody (Bioworld, Nanjing, Jiangsu, China). Target bands were detected using an enhanced electrochemiluminescence (ECL) system (Thermo-Fisher Scientific, Waltham, MA, USA).

Tumorigenicity in Vivo

MiR-138-5p or miR-NC transfected SM-MC-7721 cells were subcutaneously administered into BALB/c nude mice (Shanghai Slack Laboratory Animal Co., Ltd., Shanghai, China). The width and length of tumor xenografts were measured every week. BALB/c nude mice were sacrificed at 35 days and tumor tissues were excised. Tumor volume was calculated using the following equation: $0.5 \times \text{length} \times \text{width}^2$. This xenograft experiment was approved by the Ethics Review Committee of Zhongnan Hospital of Wuhan University.

Statistical Analysis

Results were expressed as Means \pm standard deviation (SD). Statistical differences between the two groups were analyzed using the Student's *t*-test. Comparison between multiple groups was done using the One-way ANOVA test followed by post-hoc test (Least Significant Difference). $p < 0.05$ was considered as statistically significant.

Results

MiR-138-5p Is Related to the Poor Survival of Patient With HCC

In order to study the functions of miR-138-5p in the development of HCC, we firstly analyzed the levels of miR-138-5p in normal liver samples and corresponding HCC samples using ISH assay. As demonstrated in Figure 1A, miR-138-5p positive staining was markedly lower in HCC

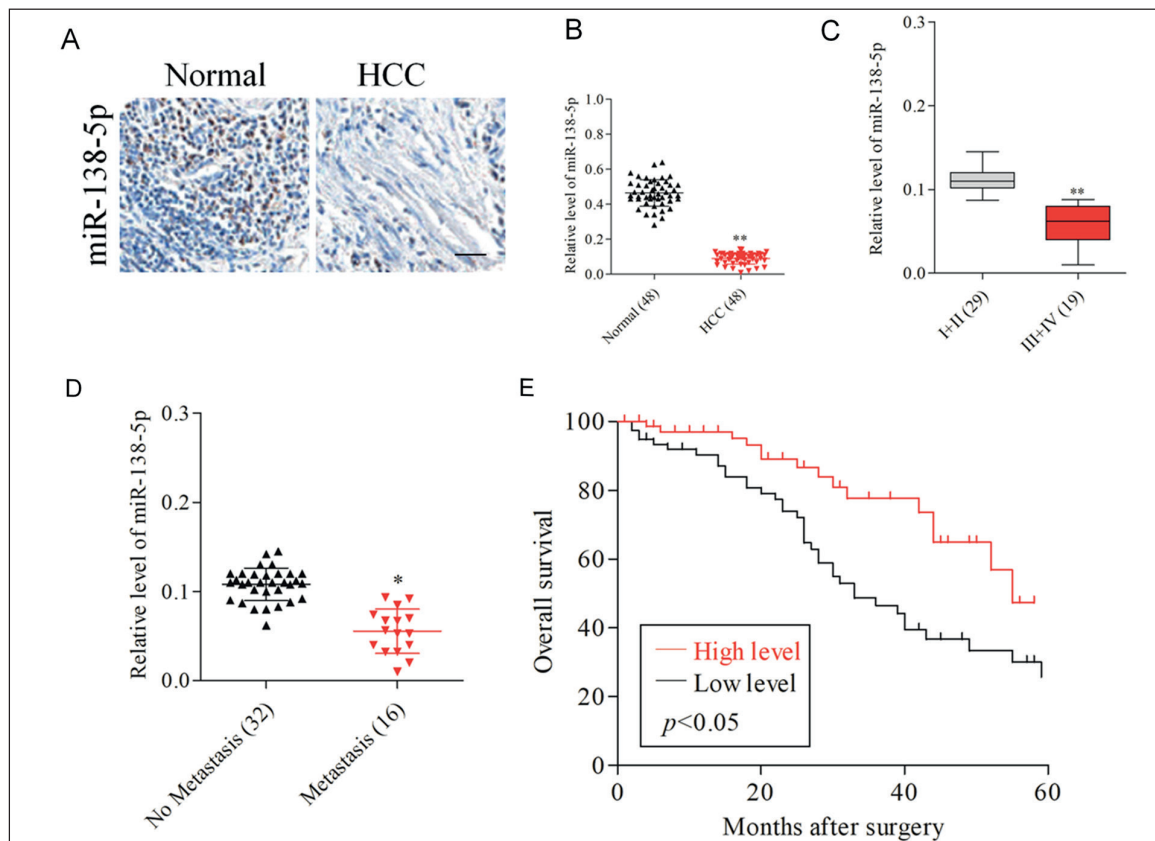


Figure 1. The relationship between miR-138-5p level in HCC tissues and clinical significance. **A.** *In situ* hybridization to detect miR-138-5p expression in 48 paired HCC and adjacent non-cancerous tissues (Normal) ($\times 200$). **B.** Quantitation of miR-138-5p was performed using qRT-PCR in 48 HCC and adjacent normal tissues. $**p < 0.01$ vs. Normal. **C-D.** miR-138-5p expression was detected in primary tumor tissues and the patients were grouped according to distant metastasis status or clinical stages. $*p < 0.05$, $**p < 0.01$ vs. I+II or No metastasis. **E.** Kaplan-Meier overall survival curves according to high and low miR-138-5p expression in 48 patients with HCC.

samples than that in the corresponding normal liver tissues. In addition, the qRT-PCR results indicated that miR-138-5p was downregulated in HCC than in normal liver tissues ($n = 48$, Figure 1B). We also observed that the expression of miR-138-5p was lower in HCC tissue from patient with distant metastasis and advanced clinical stages (Figure 1C-1D). Finally, Kaplan-Meier survival test suggested that the lower expression of miR-138-5p was connected to the poor overall survival (OS) in HCC patients (Figure 1E). All these findings indicated that miR-138-5p was strikingly downregulated and associated with the progression of HCC.

MiR-138-5p Represses HCC Cell Growth and Metastatic Ability

Among the five HCC cell lines, we found that SMMC-7721 cell line had the lowest level of miR-138-5p (Figure 2A) when compared to normal human liver cell line, LO2. Therefore, SMMC-7721 was selected for following cell growth, colony formation, invasiveness, and migration assay. SMMC-7721 cell was transfected with miR-138-5p mimics and the expression of miR-138-5p was detected by using qRT-PCR. As shown in Figure 2B, transfection of miR-138-5p mimics raised the level of miR-138-5p in SMMC-7721 cell. Next, we observed that miR-138-5p distinctly suppressed the proliferation and colony formation of SMMC-7721 cell (Figure 2C-2D). Meanwhile, transfection of miR-138-5p markedly reduced the migration capability and invasiveness of SMMC-7721 cell *in vitro* (Figure 2E-2F). Next, HCC cell line, PLC/PRF/5 was transfected with miR-138-5p inhibitor to confirm the inhibitory impact of miR-138-5p (Figure 3A). Firstly, we found that miR-138-5p inhibitor enhanced the aggressiveness phenotypes of PLC/PRF/5 cell *in vitro*, including growth (Figure 3B) and colony formation ability (Figure 3C). Meanwhile, the migration and invasion capacities of PLC/PRF/5 were also improved by miR-138-5p inhibitor (Figure 3D-3E). All these data indicated that miR-138-5p suppressed HCC cell growth, migration and invasion abilities.

FOXC1 Is a Target of miR-138-5p in HCC

To reveal the potential mechanism through which miR-138-5p modulates HCC cell aggressiveness, the downstream target of miR-138-5p was searched using bioinformatics methods (microT, RNA22, PicTar, miRTarBase, TargetScan

and miRanda). As shown in Figure 4A, two candidate genes (FOXC1 and RARA) were identified in the Venn diagram. To verify whether FOXC1 was indeed the target gene of miR-138-5p, SMMC-7721 and PLC/PRF/5 cell was transfected with miR-138-5p and we observed that miR-138-5p significantly reduced the level of FOXC1 in HCC cell (Figure 4B and 4C). Next, luciferase reporter gene assay was carried out to reveal the interaction between miR-138-5p and FOXC1. As shown in Figure 4D, miR-138-5p distinctly decreased the luciferase activity in HCC cell that was cotransfected with pmirGLO luciferase reporter carrying FOXC1-Wt, while miR-138-5p had no suppressive role on the luciferase activity in HCC cell that was cotransfected with pmirGLO luciferase reporter carrying FOXC1-Mut. Altogether, these results indicated that miR-138-5p bound with the 3'-UTR of FOXC1.

MiR-138-5p Represses HCC by Modulating FOXC1

Next, several rescue experiments were carried out to verify that FOXC1 gene was the directly target of miR-138-5p. SMMC-7721 cell was transfected with miR-138-5p alone or cotransfected miR-138-5p mimics and FOXC1. The protein expression of FOXC1 in SMMC-771 cell was reduced by miR-138-5p and recovered by cotransfection of pcDNA3.1 vector carrying FOXC1 (Figure 5A). Next, the following functional assays suggested that the colony formation and aggressive phenotypes inhibited by miR-138-5p were rescued by FOXC1 (Figure 5B-5E). Next, PLC/PRF/5 cell was transfected with miR-138-5p inhibitor (anti-miR-138-5p) alone or cotransfected anti-miR-138-5p and si-FOXC1. The protein expression of FOXC1 in PLC/PRF/5 cell was increased by anti-miR-138-5p and reduced by cotransfection of siFOXC1 (Figure 6A). Afterwords, we observed that the colony formation and aggressive phenotypes enhanced by anti-miR-138-5p were inhibited by siFOXC1 (Figure 6B-6E). Altogether, these results indicated that miR-138-5p suppressed HCC through targeting FOXC1.

MiR-138-5p Inhibits Tumor Growth of HCC Cell in Vivo

We finally explored the suppressive effects of miR-138-5p on the growth of HCC cell *in vivo*. SMMC-7721 cell was transfected with miR-138-5p or miR-NC. The upregulation of miR-138-5p

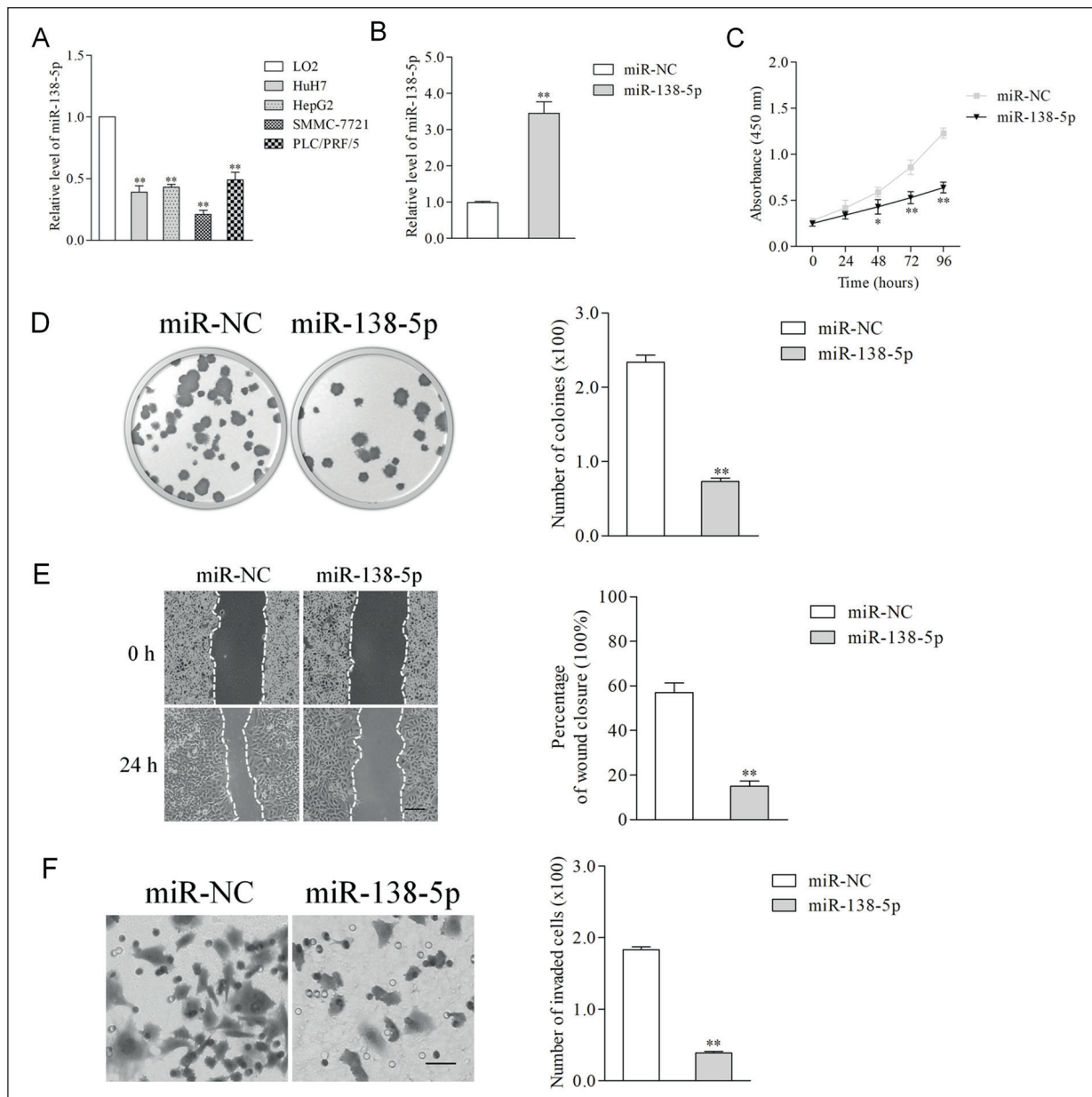


Figure 2. miR-138-5p overexpression inhibited SMMC-7721 cell proliferation, colony formation, and migration. **A.** The level of miR-138-5p in four HCC cell lines. ** $p < 0.01$ vs. LO2 cell. **B.** Quantitation of miR-138-5p level after the transfection of miR-138-5p mimic in SMMC-7721 cell line. **C.** Cell growth curve measured using CCK-8 assay after the transfection of miR-138-5p mimic in SMMC-7721 cell line. **D.** Representative images and quantitative results of colony formation were obtained after transfection with miR-138-5p mimic in SMMC-7721 cell line ($\times 200$). **E.** Representative images and quantitative results of the wound healing assay were obtained after transfection with miR-138-5p mimic in SMMC-7721 cell ($\times 200$). Scale bars represent 200 μm . **F.** Representative images and quantitative results of the Transwell assay were obtained after transfection with miR-138-5p mimic in SMMC-7721 cell ($\times 200$). ** $p < 0.01$ vs. miR-NC. Scale bars represent 100 μm .

in SMMC-7721 cell after lentiviral infection was determined by using qRT-PCR (Figure 7A). Next, SMMC-7721 cells were subcutaneously injected in BALB/c nude mice. The tumor growth curve indicated that the growth rate was significantly inhibited in miR-138-5p-overregu-

lated group (Figure 7B). Then, the tumor tissues in the two groups were dissected and weighted (Figure 7C). Moreover, tumor tissues were subjected to immunohistochemistry (IHC) assay using Ki-67 antibody. The Ki-67 staining was significantly reduced in tumors derived from

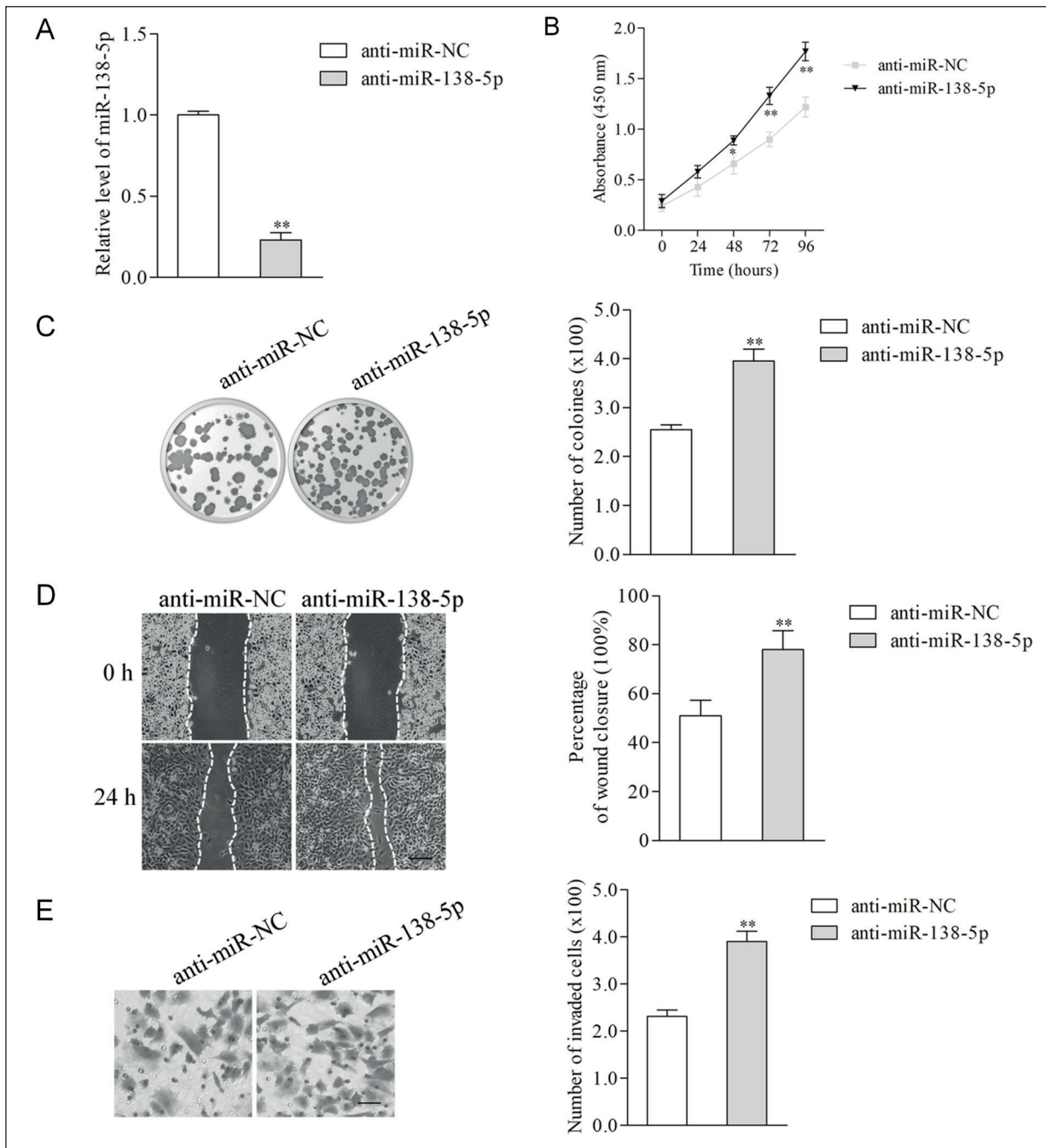


Figure 3. Repression of miR-138-5p expression significantly promoted cell growth, colony formation, and migration in PLC/PRF/5 cell. **A.** Quantitative measurement of miR-138-5p level after the transfection of miR-138-5p inhibitor in PLC/PRF/5 cell. **B.** Cell growth curve measured by CCK-8 after transfection with miR-138-5p inhibitor in PLC/PRF/5 cell. **C.** Representative images and quantitative results of colony formation were obtained after transfection with miR-138-5p inhibitor in PLC/PRF/5 cell ($\times 200$). **D.** Representative images and quantitative results of the wound healing assay were obtained after the transfection of miR-138-5p inhibitor in PLC/PRF/5 ($\times 200$). Scale bars represent 200 μm . **E.** Representative images and quantitative results of the Transwell assay were obtained after the transfection of miR-138-5p inhibitor in PLC/PRF/5 cell ($\times 200$). ** $p < 0.01$ vs. anti-miR-NC. Scale bars represent 100 μm .

miR-138-5p overexpressing SMMC-7721 cells (Figure 7D). Furthermore, a markedly decrease in FOXC1 staining was found in tumors derived

from miR-138-5p-overregulated SMMC-7721 cells compared with the staining in the miR-NC group (Figure 7 E).

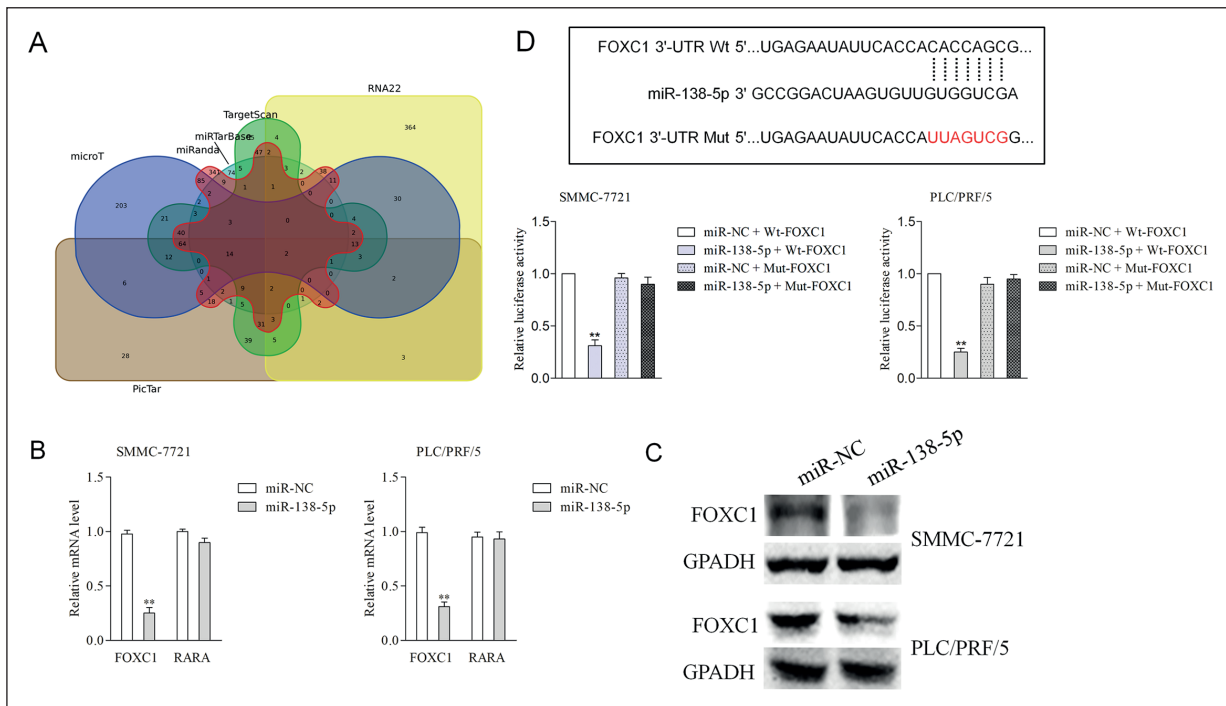


Figure 4. FOXC1 was a direct target gene of miR-138-5p. **A.** The downstream target of miR-138-5p was searched using bioinformatics methods (microT, RNA22, PicTar, miRtarBase, TargetScan and miRanda). Two candidate genes (FOXC1 and RARA) were identified in the Venn diagram. **B.** The mRNA levels of FOXC1 and RARA were measured by qRT-PCR in SMMC-7721 and PLC/PRF/5 cell. ****** $p < 0.01$ vs. miR-NC. **C.** The expression levels of FOXC1 were measured by Western blot analysis. **D.** Luciferase reporter assay. The relative luciferase activity was normalized to the Renilla luciferase activity after co-transfection of cells with miR-138-5p mimic and pmirGLO luciferase reporter containing Wt or Mut FOXC1 3'-UTR region in SMMC-7721 and PLC/PRF/5 cell. ****** $p < 0.01$ vs. miR-NC + Wt-FOXC1.

Discussion

MicroRNAs have been proved to be involved in the tumorigenesis and process of multiple tumor types⁶⁻⁹. The alteration in miR-138-5p expression has been observed in several cancers^{5,10,11}. So, miRNA-138-5p inhibits the migration, invasion and epithelial-mesenchymal transition (EMT) of breast cancer through targeting rhomboid domain-containing protein 1 (RHBDD1)¹². MiR-138-5p also represses the EMT, growth and metastasis of lung adenocarcinoma cell by modulating zinc finger E-box-binding homeobox 2 (ZEB2)¹³. In this research, we revealed that miR-138-5p was distinctly down-expressed in human HCC tissues. A low level of miR-138-5p was also observed in HCC cells lines when compared to LO2 cell. Meanwhile, the low expression of miR-138-5p was closely related to higher stage and distant metastasis of HCC. Furthermore, the patients with HCC harboring lower miR-138-5p levels showed significantly shorter overall survival than HCC patients with higher miR-138-5p

expression. These findings are in line with previous investigations, which indicate that the level of miR-138-5p is commonly down-expressed in cancers and may be closely related to HCC progression.

Plenty of miRNAs have cancer-inhibitory roles in HCC and other types of cancers. In particular, miR-525-3p induces the invasion and migration of HCC cell through modulating zinc finger protein 395 (ZNF395)¹⁴. MiRNA-302a/d represses the self-renewal ability of liver cancer stem cell through regulating the E2F Transcription Factor 7/Serine/Threonine Kinase (E2F7/AKT) axis¹⁵. In this research, we proved that transfection of miR-138-5p repressed the cell proliferation and colony formation of HCC cells. Meanwhile, upregulation of miR-138-5p restrained the migration and invasion capacities of HCC cells *in vitro*. Nevertheless, down-regulation of miR-138-5p caused completely opposite results. Recent reports have indicated that miR-138-5p is strikingly downregulated in gastric cancer (GC) and pancreatic cancer^{16,17}. In human

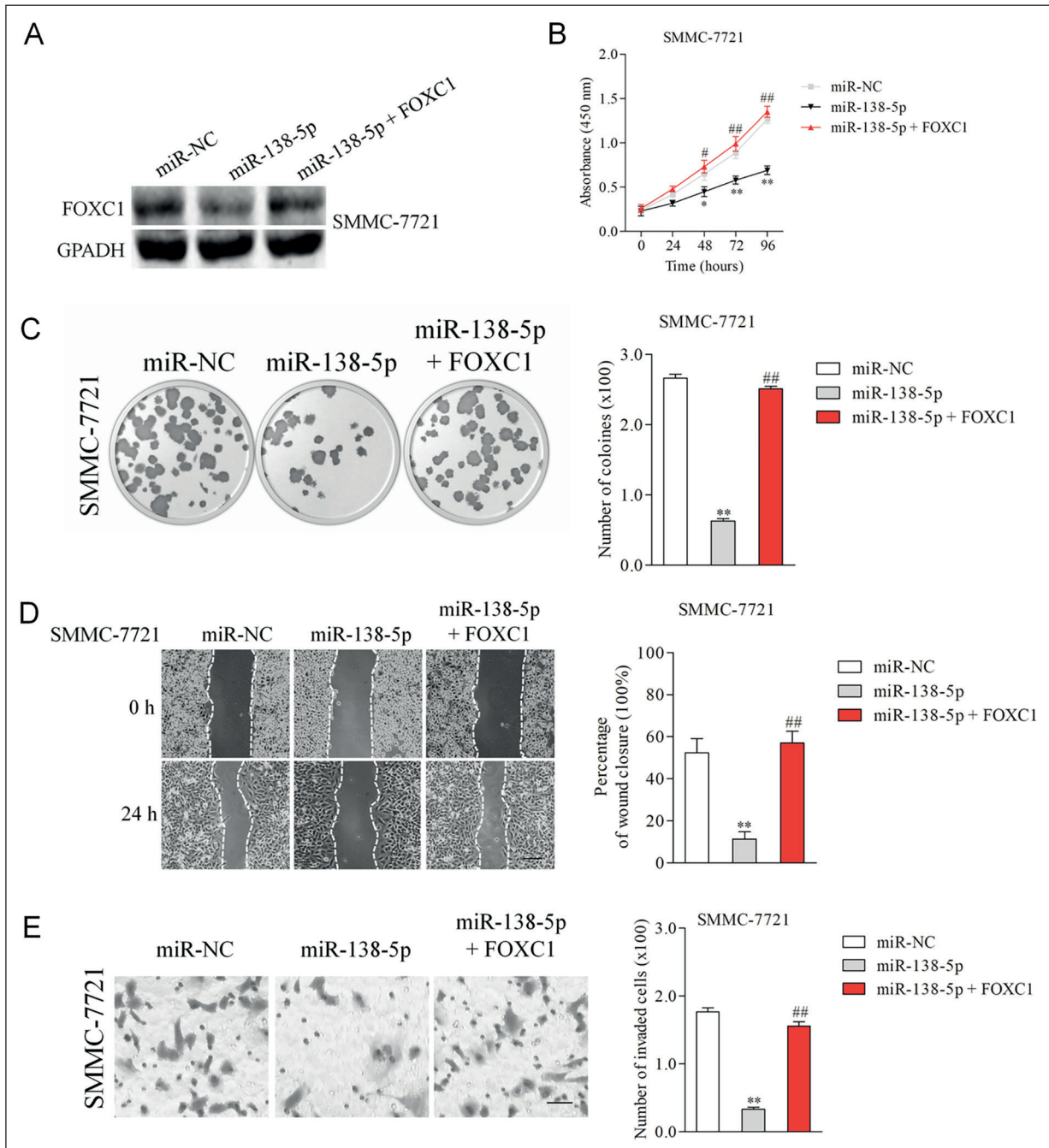


Figure 5. MiR-138-5p repressed HCC by modulating FOXC1. **A.** The protein level of FOXC1 in SMMC-7721 with co-transfection of miR-138-5p mimics and pcDNA3.1 vector containing FOXC1. **B-C.** Cell proliferation and colony formation assay of co-transfection cell with miR-138-5p mimics and FOXC1 plasmid ($\times 200$). **D-E.** Wound healing and Transwell assay of co-transfection cell with miR-138-5p mimics and FOXC1 plasmid ($\times 200$). Scale bars represent 100 μm . $**p < 0.01$ vs. miR-NC, $##p < 0.01$ vs. miR-138-5p.

retinoblastoma, miR-138-5p functions as a cancer-suppressive miRNA through modulating pyruvate dehydrogenase kinase 1 (PDHA1)¹¹. MiR-138-5p is also down-expressed in colorectal carcinoma (CRC) and is related to the advanced

stage and poor clinical outcomes of patients¹⁸. All observations support our findings that miR-138-5p serves as a cancer suppressive miRNA.

MiRNAs are primarily processed by the RNA-mediated interference machinery to trig-

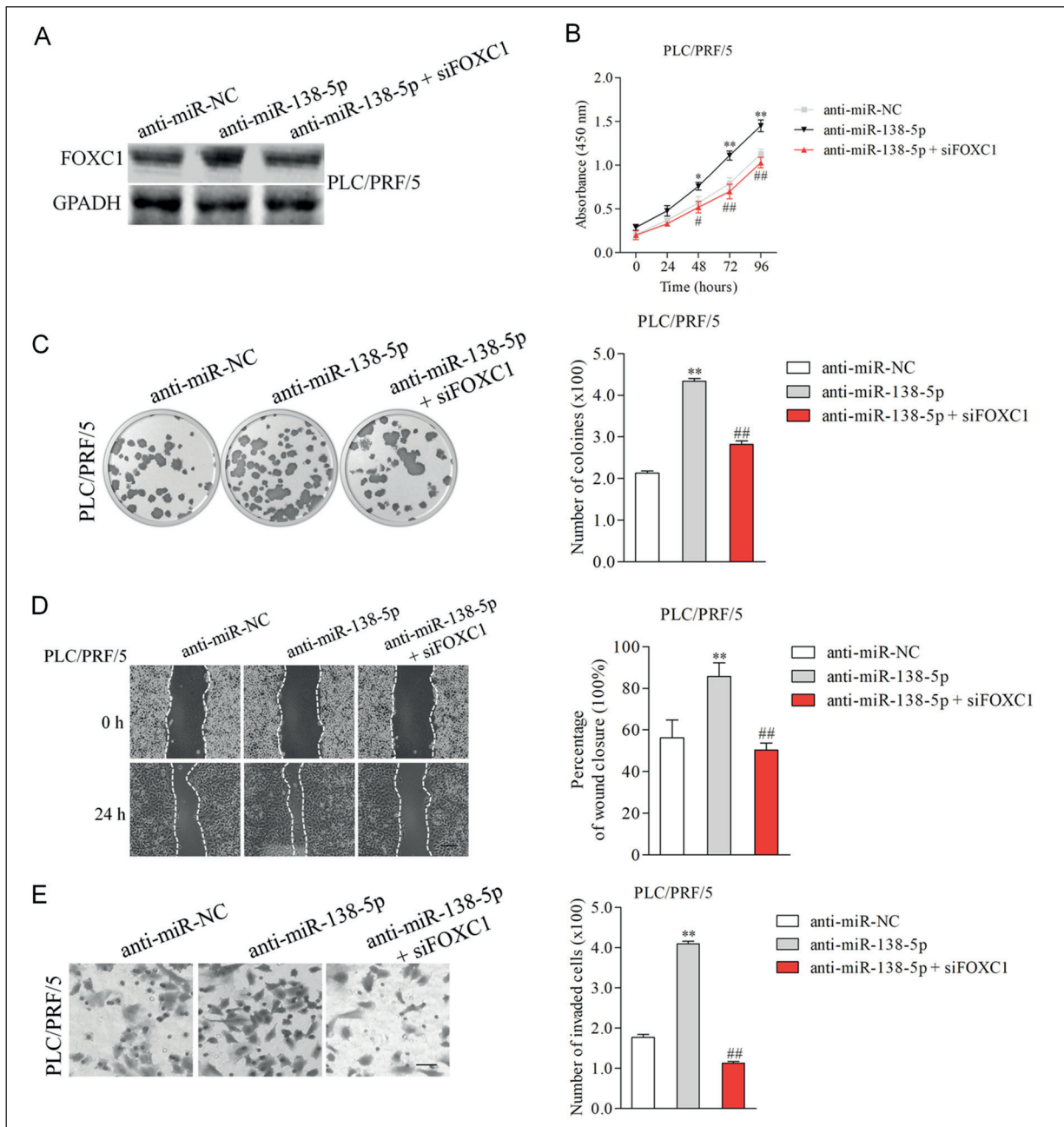


Figure 6. Rescue assays were performed to confirm that FOXC1 is the functional target of miR-138-5p. **A.** The protein level of FOXC1 in PLC/PRF/5 with co-transfection of miR-138-5p inhibitor (anti-miR-138-5p) and siFOXCI. **B-C.** Cell proliferation and colony formation assay of co-transfection cell with anti-miR-138-5p and siFOXCI ($\times 200$). **D-E.** Wound healing and Transwell assay of co-transfection cell with anti-miR-138-5p and siFOXCI ($\times 200$). Scale bars represent 100 μm . $**p < 0.01$ vs. anti-miR-NC, $##p < 0.01$ vs. anti-miR-138-5p.

ger partial or complete target gene mRNA degradation^{19,20}. Our bioinformatics analysis indicated that FOXC1 was a potential target gene of miR-138-5p. The result of luciferase reporter gene assay further indicated that miR-138-5p directly interacted with the 3'-UTR of FOXC1.

FOXC1 is a member of the forkhead box family of transcription factors (TFs) and has been shown to have a critical role in embryogenesis, differentiation, and angiogenesis. Recently, FOXC1 has been found overexpressed in cancers²¹⁻²⁴. In primary hepatocellular carcinoma, FOXC1 con-

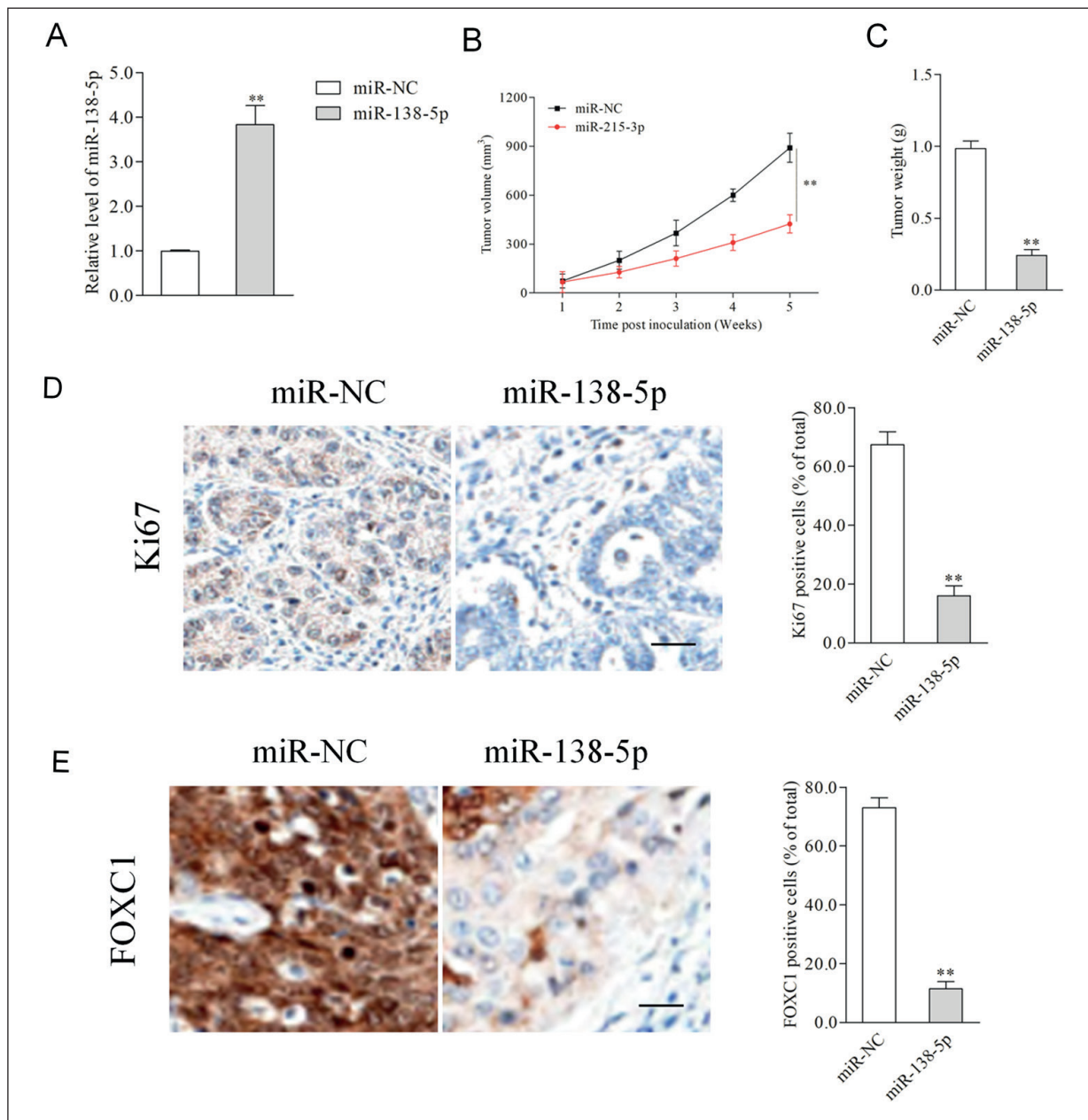


Figure 7. miR-138-5p suppressed tumor growth of HCC cell *in vivo*. **A.** The level of miR-138-5p in miR-138-5p mimics transfected SMMC-7721 cell was assessed using qRT-PCR assay. **B-C.** MiR-138-5p transfected SMMC-7721 cells were subcutaneously injected into nude mice. The tumor volumes and tumor weights were analyzed. **D-E.** Immunohistochemistry of Ki67 and FOXC1 in tumor tissues dissected from nude mice treated with miR-138-5p or miR-NC transfected SMMC-7721 cells ($\times 200$). Scale bars represent 100 μm . ** $p < 0.01$ vs. miR-NC.

tributes to the microvascular invasion of cancer cell through regulating EMT²⁵. In our study, the expressions of FOXC1 were markedly reduced by miR-138-5p in HCC cells as demonstrated by qRT-PCR and Western blotting assays.

To characterize the detailed roles of miR-138-5p/FOXC1 axis in HCC progression, HCC cell

was transfected with miR-138-5p and pcDNA3.1 vector containing FOXC1. The several rescue experiments indicated that re-expression of FOXC1 restored the growth and metastatic-related traits of HCC cells that were impaired by miR-138-5p. As expected, FOXC1 silencing weakened the growth and metastatic-related traits of HCC cells

that were enhanced by miR-138-5p inhibitor. All these observations suggested that miR-138-5p might inhibit HCC growth and aggressiveness through regulating FOXC1. Finally, we proved that transfection of miR-138-5p significantly inhibited HCC cell growth *in vivo*. The Ki-67 staining was markedly reduced in the tumor tissue formed by miR-138-5p-overexpressing HCC cell. The immunohistochemistry (IHC) staining results further showed that FOXC1 staining in xenograft tumors of the miR-138-5p transfected HCC group were significantly reduced than that in tumor tissue derived from miR-NC transfected cell, indicating that the growth of HCC cells and the expression of FOXC1 were decreased by miR-138-5p *in vivo*.

Conclusions

In short, our findings indicate that miR-138-5p is down-expressed in human HCC and miR-138-5p might act as a potential predictor for the clinical outcomes of patients with HCC. Moreover, we demonstrate that miR-138-5p possesses the inhibitory effects in HCC growth and aggressive phenotypes through modulating its target gene, FOXC1. Our data suggest that miR-138-5p serves as an antioncogene in HCC and reveals the crucial role of miR-138-5p /FOXC1 in the progression of HCC.

Conflict of Interest

The Authors declare that they have no conflict of interests.

References

- XIE BH, HE X, HUA RX, ZHANG B, TAN GS, XIONG SQ, LIU LS, CHEN W, YANG JY, WANG XN, LI HP. Mir-765 promotes cell proliferation by downregulating INP-P4B expression in human hepatocellular carcinoma. *Cancer Biomark* 2016; 16: 405-413.
- LIANG S, ZHANG N, DENG Y, CHEN L, ZHANG Y, ZHENG Z, LUO W, LV Z, LI S, XU T. miR-663b promotes tumor cell proliferation, migration and invasion in nasopharyngeal carcinoma through targeting TUSC2. *Exp Ther Med* 2017; 14: 1095-1103.
- ZHAO HJ, REN LL, WANG ZH, SUN TT, YU YN, WANG YC, YAN TT, ZOU W, HE J, ZHANG Y, HONG J, FANG JY. MiR-194 deregulation contributes to colorectal carcinogenesis via targeting AKT2 pathway. *Theranostics* 2014; 4: 1193-1208.
- HE Z, YI J, LIU X, CHEN J, HAN S, JIN L, CHEN L, SONG H. MiR-143-3p functions as a tumor suppressor by regulating cell proliferation, invasion and epithelial-mesenchymal transition by targeting QKI-5 in esophageal squamous cell carcinoma. *Mol Cancer* 2016; 15: 51.
- YANG R, LIU M, LIANG H, GUO S, GUO X, YUAN M, LIAN H, YAN X, ZHANG S, CHEN X, FANG F, GUO H, ZHANG C. miR-138-5p contributes to cell proliferation and invasion by targeting Survivin in bladder cancer cells. *Mol Cancer* 2016; 15: 82.
- LIANG X, LI Z, MEN Q, LI Y, LI H, CHONG T. miR-326 functions as a tumor suppressor in human prostatic carcinoma by targeting *Mucin1*. *Biomed Pharmacother* 2018; 108: 574-583.
- RIQUELME I, TAPIA O, LEAL P, SANDOVAL A, VARGA MG, LETELIER P, BUCHEGGER K, BIZAMA C, ESPINOZA JA, PEEK RM, ARAYA JC, ROA JC. miR-101-2, miR-125b-2 and miR-451a act as potential tumor suppressors in gastric cancer through regulation of the PI3K/AKT/mTOR pathway. *Cell Oncol (Dordr)* 2016; 39: 23-33.
- CHEN ML, LIANG LS, WANG XK. miR-200c inhibits invasion and migration in human colon cancer cells SW480/620 by targeting ZEB1. *Clin Exp Metastasis* 2012; 29: 457-469.
- LUO J, CHEN J, HE L. mir-129-5p attenuates irradiation-induced autophagy and decreases radioresistance of breast cancer cells by targeting HMGB1. *Med Sci Monit* 2015; 21: 4122-4129.
- GAO Y, FAN X, LI W, PING W, DENG Y, FU X. miR-138-5p reverses gefitinib resistance in non-small cell lung cancer cells via negatively regulating G protein-coupled receptor 124. *Biochem Biophys Res Commun* 2014; 446: 179-186.
- WANG Z, YAO YJ, ZHENG F, GUAN Z, ZHANG L, DONG N, QIN WJ. Mir-138-5p acts as a tumor suppressor by targeting pyruvate dehydrogenase kinase 1 in human retinoblastoma. *Eur Rev Med Pharmacol Sci* 2017; 21: 5624-5629.
- ZHAO C, LING X, LI X, HOU X, ZHAO D. MicroRNA-138-5p inhibits cell migration, invasion and EMT in breast cancer by directly targeting RHBDD1. *Breast Cancer* 2019; 26: 817-825.
- ZHU D, GU L, LI Z, JIN W, LU Q, REN T. MiR-138-5p suppresses lung adenocarcinoma cell epithelial-mesenchymal transition, proliferation and metastasis by targeting ZEB2. *Pathol Res Pract* 2019; 215: 861-872.
- PANG F, ZHA R, ZHAO Y, WANG Q, CHEN D, ZHANG Z, CHEN T, YAO M, GU J, HE X. MiR-525-3p enhances the migration and invasion of liver cancer cells by downregulating ZNF395. *PLoS One* 2014; 9: e90867.
- MA YS, LV ZW, YU F, CHANG ZY, CONG XL, ZHONG XM, LU GX, ZHU J, FU D. MicroRNA-302a/d inhibits the self-renewal capability and cell cycle entry of liver cancer stem cells by targeting the E2F7/AKT axis. *J Exp Clin Cancer Res* 2018; 37: 252.
- WANG Y, ZHANG H, GE S, FAN Q, ZHOU L, LI H, BAI M, NING T, LIU R, WANG X, DENG T, ZHANG L, YING G, BA

- Y. Effects of miR1385p and miR2045p on the migration and proliferation of gastric cancer cells by targeting EGFR. *Oncol Rep* 2018; 39: 2624-2634.
- 17) TIAN S, GUO X, YU C, SUN C, JIANG J. miR-138-5p suppresses autophagy in pancreatic cancer by targeting SIRT1. *Oncotarget* 2017; 8: 11071-11082.
 - 18) ZHAO L, YU H, YI S, PENG X, SU P, XIAO Z, LIU R, TANG A, LI X, LIU F, SHEN S. The tumor suppressor miR-138-5p targets PD-L1 in colorectal cancer. *Oncotarget* 2016; 7: 45370-45384.
 - 19) WANG JM, JU BH, PAN CJ, GU Y, LI MQ, SUN L, XU YY, YIN LR. MiR-214 inhibits cell migration, invasion and promotes the drug sensitivity in human cervical cancer by targeting FOXM1. *Am J Transl Res* 2017; 9: 3541-3557.
 - 20) MA DN, CHAI ZT, ZHU XD, ZHANG N, ZHAN DH, YE BG, WANG CH, QIN CD, ZHAO YM, ZHU WP, CAO MQ, GAO DM, SUN HC, TANG ZY. MicroRNA-26a suppresses epithelial-mesenchymal transition in human hepatocellular carcinoma by repressing enhancer of zeste homolog 2. *J Hematol Oncol* 2016; 9: 1.
 - 21) SIZEMORE ST, KERI RA. The forkhead box transcription factor FOXC1 promotes breast cancer invasion by inducing matrix metalloprotease 7 (MMP7) expression. *J Biol Chem* 2012; 287: 24631-24640.
 - 22) HAN B, ZHOU B, QU Y, GAO B, XU Y, CHUNG S, TANAKA H, YANG W, GIULIANO AE, CUI X. FOXC1-induced non-canonical WNT5A-MMP7 signaling regulates invasiveness in triple-negative breast cancer. *Oncogene* 2018; 37: 1399-1408.
 - 23) ZHU X, WEI L, BAI Y, WU S, HAN S. FoxC1 promotes epithelial-mesenchymal transition through PBX1 dependent transactivation of ZEB2 in esophageal cancer. *Am J Cancer Res* 2017; 7: 1642-1653.
 - 24) CAO S, WANG Z, GAO X, HE W, CAI Y, CHEN H, XU R. FOXC1 induces cancer stem cell-like properties through upregulation of beta-catenin in NSCLC. *J Exp Clin Cancer Res* 2018; 37: 220.
 - 25) XU ZY, DING SM, ZHOU L, XIE HY, CHEN KJ, ZHANG W, XING CY, GUO HJ, ZHENG SS. FOXC1 contributes to microvascular invasion in primary hepatocellular carcinoma via regulating epithelial-mesenchymal transition. *Int J Biol Sci* 2012; 8: 1130-1141.